Green Synthesis, Characterization and Cytotoxic Activity of Gold and Silver Nanoparticles Using Kaempferol-3′-sulfonate

[1]Xin–Bin Yang*, [1]Chun–Mei Wang, [2]Yu Huang
[1]*Rongchang Campus, Southwest University, Chongqing 402460, P. R.China.*
[2]*Pharmacy College, Ningxia Medical University, Yinchuan 750004, P. R. China.*
yangxbqq@126.com*; 676071388@qq.com; huangyunxmu@163.com

(Received on 7th Jan 2019, accepted in revised form 2nd August 2019)

Summary: Gold nanoparticles (AuNPs) and silver nanoparticles (AgNPs) were synthesized by using water-soluble Kaempferol–3′–sulfonate acid sodium (KS) alone as the reducing agent. The UV-vis spectra confirmed the formation of the ks-AuNPs and ks-AgNPs which were stable for up to 3 months without any other stabilizing agents at room temperature. The TEM studies exhibited monodispersed and mainly spherical nanoparticles with the size in the range of 15-30 nm and 20-50 nm for ks-AuNPs and ks-AgNPs, respectively. The XRD revealed crystallinity of nanoparticles. The chemical state of Au and Ag on the surface of nanoparticles was analyzed by XPS. The FTIR analysis indicated that the hydroxyl of KS were responsible for the reduction of Au^{3+} and Ag^{+} to ks-AuNPs and ks-AgNPs, respectively. Cytotoxic activity of ks-AuNPs and ks-AgNPs on MCF-7 cells is higher than the KS.

Key words: Kaempferol-3′-sulfonate acid sodium; gold nanoparticles; sliver nanoparticles; cytotoxic activity

Introduction

AuNPs and AgNPs show great promise in biomedicine due to their biological applications such as anticancer, antimicrobial, molecular imaging, gene therapy, DNA analysis and drug delivery [1-9]. However, many chemical synthetic methods of AuNPs and AgNPs using sodium borohydride, CTAB and organic solvents, etc were harmful to the environment and human health [10]. Therefore, searching for an efficient and environmentally friendly synthetic method of AuNPs and AgNPs is of great importance.

In order to develop novel green synthetic method of AuNPs and AgNPs, a new strategy has been adopted by employing different types of plant extracts containing natural biomolecules such as tannic acid, flavanoids, curcumin, polyphonenols as reducing agent as well as stabilizing / capping agent during the last few decades [11-17]. However, it is unclear which active component is responsible for the reduction. Recently, it has been reported that AuNPs prepared using pure curcumin, quercetin as reductants exhibit excellent antibacterial, anticancer and biocompatibity [18, 19].

Kaempferol (3, 3′, 5, 7–tetrahydroxyflavone, Kae), an abundant natural flavonoids, is found in berries, tea, Brassica and many traditional Chinese herbal medicines. It has been demonstrated to possess potential antimicrobial, antioxidant, anti–inflammatory and anticancer properties [20-22]. It was also reported that Kae had significantly less cytotoxicity than 5-fluorouracil on normal human pancreatic ductal

property of Kae limited its clinical applications. In previous work, we synthesized water soluble kaempferol–3′–sulfonate acid sodium (scheme 1) and evaluated the protective effects of KS on human vascular smooth muscle cells injury induced by hydrogen peroxide [24]. However, to the best of our knowledge, there are no reports on synthesis, characterization and cytotoxic activities of AuNPs and AgNPs conjugated water soluble KS. In this work, we report the synthesis of AuNPs and AgNPs by using water as solvent and KS as the reducing agent. Furthermore, the cytotoxic activities o of AuNPs and AgNPs on MCF-7 cells were also investigated.

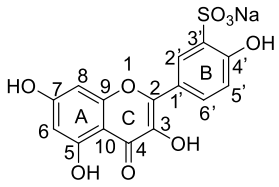

Scheme-1: kaempferol–3′–sulfonic acid sodium.

Experimental

Materials

The KS was synthesized according to the reference [24]. The other chemicals were analytical grades and used without further purification. Hydrogen tetrachloroaurate ($HAuCl_4 \cdot 3H_2O$) and silver nitrate ($AgNO_3$) were purchased from Shanghai Aladdin

***To whom all correspondence should be addressed.**

KS mediated synthesis of ks-AuNPs and ks-AgNPs

Aqueous stock solution of $HAuCl_4$, $AgNO_3$, and KS were prepared using ultrapure water, respectively. 0.4 mM of $HAuCl_4$ solution was added to 0.2 mM of KS solution at molar ratio of 2:1 for the synthesis of ks-AuNPs, and 0.8 mM of $AgNO_3$ solution was added to 0.2 mM of KS solution at molar ratio of 4:1 for the synthesis of ks-AgNPs. The reaction mixture was shaken well at room temperature and monitored using UV–Vis spectroscopy. The reaction mixture was centrifuged at 3000 rpm for 30 min. The nanoparticles obtained were washed three times with ultrapure water for further use. XRD, FTIR and XPS measurements of ks-AuNPs and ks-AgNPs were freeze dried to obtain dry powder. The effects of reaction time and stability of ks-AuNPs and ks-AgNPs were analyzed, respectively.

Characterization of ks-AuNPs and ks-AgNPs

UV–Visible spectra were measured on TU-1901 spectrophotometer (Beijing Purkinje General Insrrument Co., LTD, CHN). The FT-IR spectra were recorded in a Nicolet iS50 FT-IR spectrometer (Thermo Fisher Scientific, USA) as KBr pellets in the range of 4,000 cm^{-1} - 400 cm^{-1}. The X-ray diffraction (XRD) pattern of nanoparticles was studied by using D8 Advance instrument (Bruker, GE) an operating voltage of 40 kV and a current of 30 mA with Cukα1 radiation (wavelength = 1.54056 Å). The morphology and size were determined by transmission electron microscopy (TEM) in FEI Tecnai G2 F20 instrument (FET, USA) at accelerating voltage of 200 kV. The surface chemistry of nanoparticles was investigated by XPS in ESCALAB 250Xi instrument (Thermo Fisher Scientific, USA).

Cytotoxic assay of ks-AuNPs and ks-AgNPs on MCF-7 cells

Cytotoxic effects of synthesized nanoparticles on MCF-7 were assessed by CCK-8 method. The cells seeded in 96 well plates at density of 6500 cells per well and incubated for 24 h at 37 °C in a water-atmosphere (5% CO_2). The cells were treated with various concentrations of ks-AuNPs and ks-AgNPs from 0.05 to 0.25 mM for 48 h at 37 °C in a water-atmosphere (5% CO_2), and the cells were also treated with various concentrations of KS from 0.2 to 1 mM for evaluating the cytotoxicity of KS alone. Then, a freshly diluted CCK-8 solution was added to each well for another 1.5h. Absorbance was measured by Thermo, Multiskan MK3 at 450 nm. The calculated IC_{50} which inhibits growth of 50% of treated cells relative to control cells was calculated as the concentration of tested compound by linear fitting.

Results and Discussions

UV-vis spectroscopy analysis of ks-AuNPs and ks-AgNPs

The formation of ks-AuNPs was confirmed by the color change phenomena when the KS was mixed with the aqueous $HAuCl_4$ at room temperature. Fig.1A showed the optical photograph of pure KS (a), $HAuCl_4$ (b) and mixture of KS with $HAuCl_4$ (c). The appearance of purple color confirmed the formation of ks-AuNPs after reaction of KS with $HAuCl_4$. The formation of ks-AuNPs was monitored by UV-vis spectroscopy and presented in Fig.1B. A strong surface plasmon resonance (SPR) absorbance band at about 536 nm confirmed the formation of ks-AuNPs. The SPR absorbance band was occurred due to the collective electron oscillation around the surface of the particles. The results indicated that the purple color of ks-AuNPs solution could be attributed to the excitation of surface plasmon resonance [25-27]. Fig.1C indicated the time dependent in the formation of ks-AuNPs. The peak of KS at 364 nm disappeared completely with the appearance of the peak at 536 nm within 10 min after the addition of $HAuCl_4$ to KS solution. The intensity of SPR peak increased from 0 to 50 min indicating the formation of more nanoparticles. The stability of ks-AuNPs was studied for a period of 3 months (Fig.1D). The color of ks-AuNPs solution remained purple color and there was no significant shift in the SPR peak within 3 months. The results indicated that the ks-AuNPs formed were stable. The stability of ks-AuNPs may be due to electrostatic repulsion and the protection by the KS which act as stabilizing/capping agent. Similarly, the appearance of intense yellow color confirmed the formation of AgNPs by the reaction between $AgNO_3$ solution and KS (Fig.2A). A strong surface plasmon resonance (SPR) peak at about 440nm confirmed the formation of ks-AgNPs (Fig.2B) [28]. Fig.2C exhibited the variation in intensity of SPR peak of ks-AgNPs from 0 to 4 h. Moreover, Fig.2D indicated that the ks-AgNPs were also stable within 3 months.

Transmission electron microscopy (TEM) analysis of ks-AuNPs and ks-AgNPs

The size and shape of synthesized nanoparticles were investigated by transmission electron microscopy (TEM) and presented in Fig.3A and B. TEM images of ks-AuNPs indicated that the nanoparticles were highly monodispersed and mainly spherical in shape. The size of ks-AuNPs ranged between 15 and 30 nm. Similarly, synthesized AgNPs are large spherical in shape and are well dispersed without aggregation. The size of ks-AgNPs ranged between 20 and 50 nm.

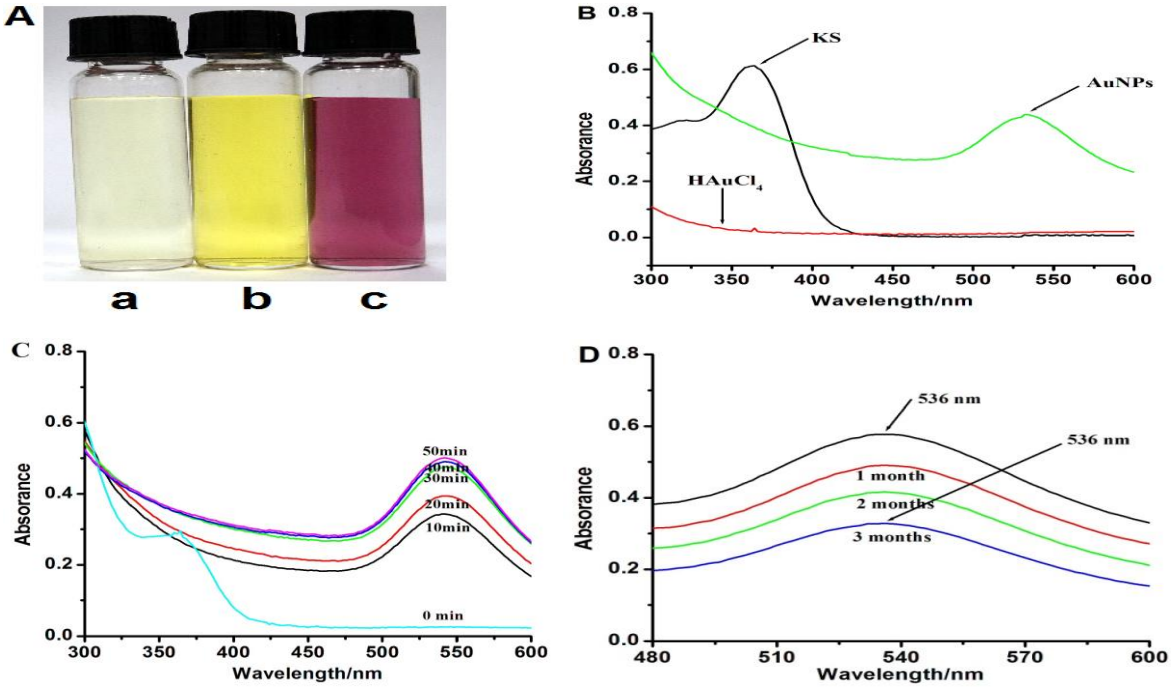

Fig. 1: A: (a) KS (b) $HAuCl_4$ (c) after the addition of $HAuCl_4$ to KS solution. B: UV-Vis absorption spectra of ks-AuNPs synthesized from KS. C: UV-Vis absorption spectra of the formation of ks-AuNPs at 0, 10, 20, 30, 40, and 50 min, respectively. D: UV-Vis absorption spectra showing the stability of ks-AuNPs for a period of 3 months.

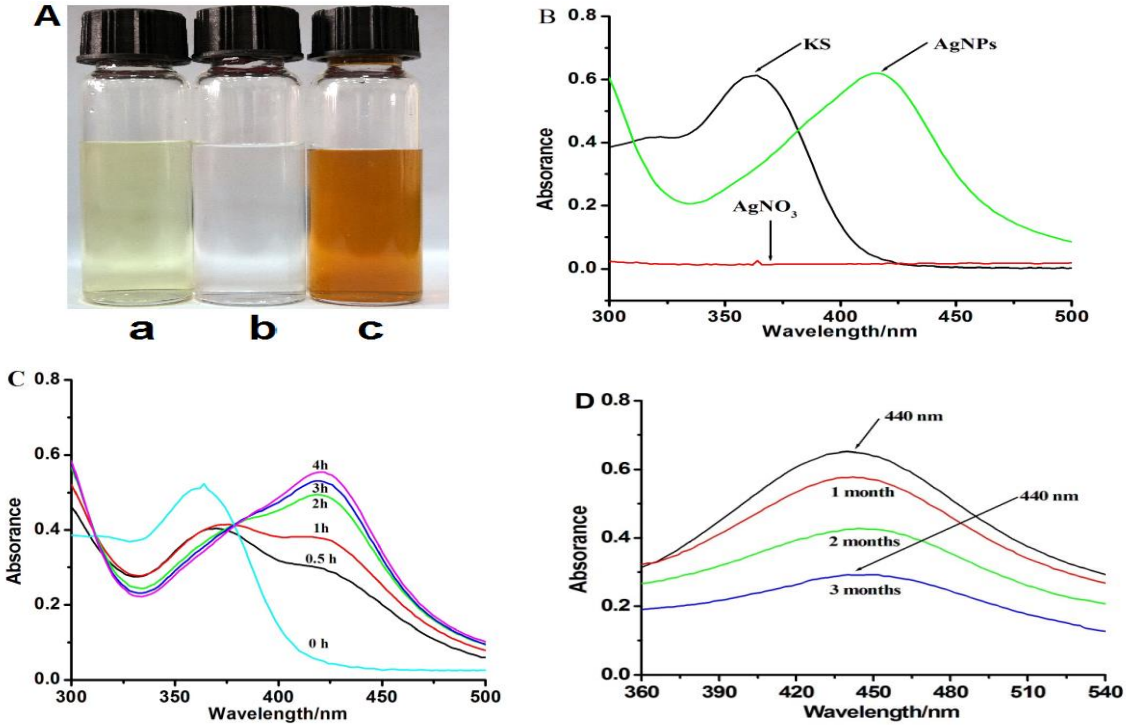

Fig. 2: A: (a) KS (b) $AgNO_3$ (c) after the addition of $AgNO_3$ to KS solution. B: UV-Vis absorption spectra of ks-AgNPs synthesized from KS. C: UV-Vis absorption spectra of the formation of ks-AgNPs at 0, 0.5, 1, 2, 3, and 4 h, respectively. D: UV-Vis absorption spectra showing the stability of ks-AgNPs for a period of 3 months.

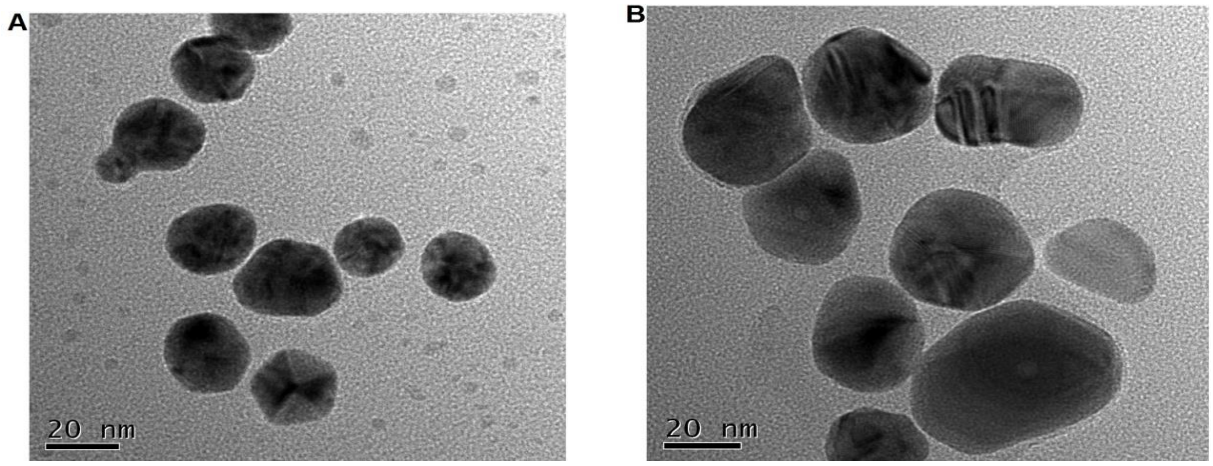

Fig. 3: TEM image of ks-AuNPs (A) and ks-AgNPs (B) obtained from KS.

X-ray diffreaction (XRD) analysis of ks-AuNPs and ks-AgNPs

The crystal structures of synthesized nanoparticles were analyzed by XRD spectra. The XRD spectrum of ks-AuNPs showed four main characteristic diffraction peaks positioned at 2θ = 38.1976, 44.4004, 64.6618 and 77.5572 degrees corresponding to the (111), (200), (220) and (311) Bragg reflections of face centered cubic structure of gold (Fig.4A). The four diffraction peaks were matched with the standard database files of gold (JCPDS file no. 04-0784). The XRD result indicated that pure crystalline gold was obtained by using KS as reducing agent. The XRD patterns of ks-AgNPs were shown in Fig. 4B. Four characteristic diffraction peaks positioned at 2θ = 38.2384, 44.3800, 64.5802 and 77.5164 degrees, corresponding to the (111), (200), (220) and (311) planes of the face centered cubic structure of silver. This was similar to JCPDS file no. 04-0783 indicating the good crystalline nature of synthesized ks-AgNPs. The average crystalline size of synthesized nanoparticles was calculated using the Debye-Scherrer equation given as $d = 0.9\lambda/\beta \cos\theta$, where d is the average crystalline size, λ is wavelength of X-ray, β is the full width at half maximum intensity of the diffraction peak of (111) Brag reflection and θ is the diffraction angle. The average size of ks-AuNPs and ks-AgNPs was found to be 21.8 and 33.2 nm, respectively.

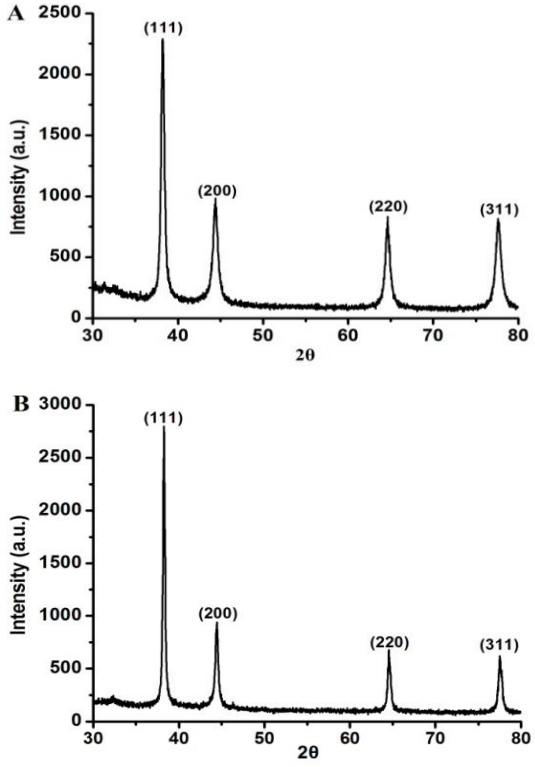

Fig. 4: X-ray diffreaction (XRD) spectra of synthesized ks-AuNPs (A) and ks-AgNPs (B).

X-ray photoelectron spectroscopy (XPS) analysis of ks-AuNPs and ks-AgNPs

The chemical environment of ks-AuNPs and ks-AgNPs was investigated by XPS and presented in Fig. 5. The binding energy peaks of Au

($4f_{5/2}$) and Au ($4f_{7/2}$) were found at around 88 eV and 84.4 eV in Fig.5A, confirming the presence of metallic Au (0) in ks-AuNPs [29-31]. Similarly, Fig.5B showed binding energy peaks at about 374.4 eV and 368.4 eV corresponding to the spin-orbit splitting components Ag ($3d_{3/2}$) and Ag ($3d_{5/2}$), which indicated the formation of metallic Ag (0) in ks-AgNPs [32].

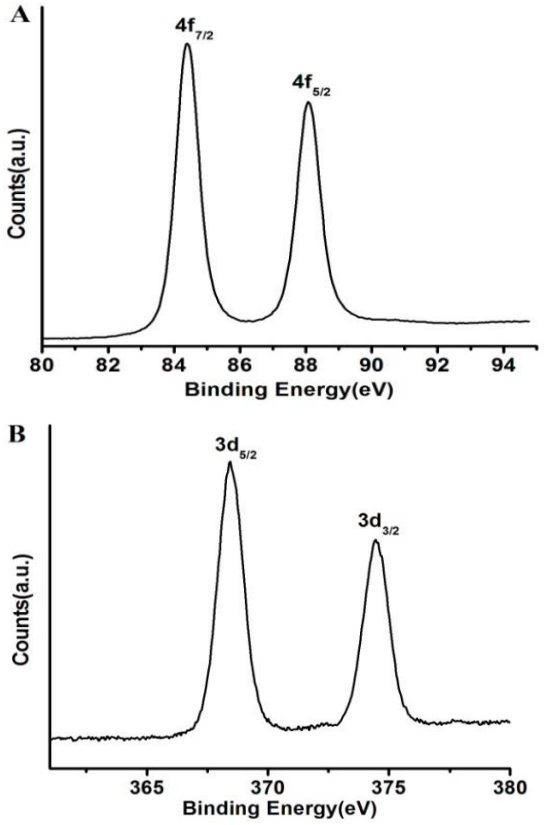

Fig. 5: X-ray photoelectron spectroscopy (XPS) of synthesized ks-AuNPs (A) and ks-AgNPs (B).

FTIR spectral analysis of ks-AuNPs and ks-AgNPs

FTIR measurements were used to identify the potential functional groups of KS that were responsible for the reduction of Au^{3+} and Ag^{+} to ks-AuNPs and ks-AgNPs, respectively. The FTIR spectra of synthesized nanoparticles were shown in Fig. 6A and 6B. The band at 1229 cm^{-1} and 1657 cm^{-1} corresponding to the plane bending of C–OH and stretch vibrations of C=O in KS were absent in ks-AuNPs and ks-AgNPs which suggested the interactions of Au^{3+} and Ag^{+} with these sites of KS, respectively. Additionally, the band at 3273 cm^{-1} corresponding to the stretch vibrations of O–H in KS was shifted towards shorter frequency 3140 cm^{-1} confirming the role –OH groups as reducing agent for the formation of ks-AuNPs and ks-AgNPs [33]. The bands at 1129 cm^{-1}, 1400 cm^{-1} and 1628 cm^{-1} assigned to the stretch vibrations of S=O and aromatic vibrations of C-H and C=C in ks-AuNPs and ks-AgNPs were similar to KS [24].

Cytotoxic effects of ks-AuNPs and ks-AgNPs on MCF-7 cell lines

Cytotoxic effects of ks-AuNPs and ks-AgNPs on MCF-7 cells were investigated by CCK-8 assay. Fig.7(B)-(D) showed the cytotoxic activity of ks-AuNPs, ks-AgNPs and KS on MCF-7 cells in the concentration of 0.2 mM after 48h incubation, respectively. The IC_{50} values of the experiment were analyzed by linear fitting. The IC_{50} values of ks-AuNPs and ks-AgNPs were found to be 0.145 mM and 0.20 mM for 48 h, respectively. However, the IC_{50} value was 0.80 mM when MCF-7 cells were treated with pure KS for 48 h. The results indicated that ks-AuNPs and ks-AgNPs had higher cytotoxic potential than KS alone.

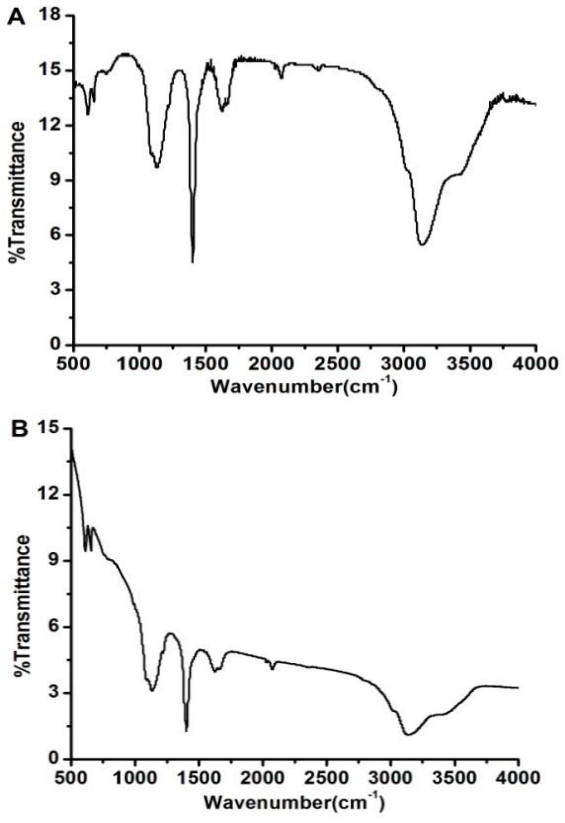

Fig. 6: FTIR spectra of synthesized ks-AuNPs (A) and ks-AgNPs (B).

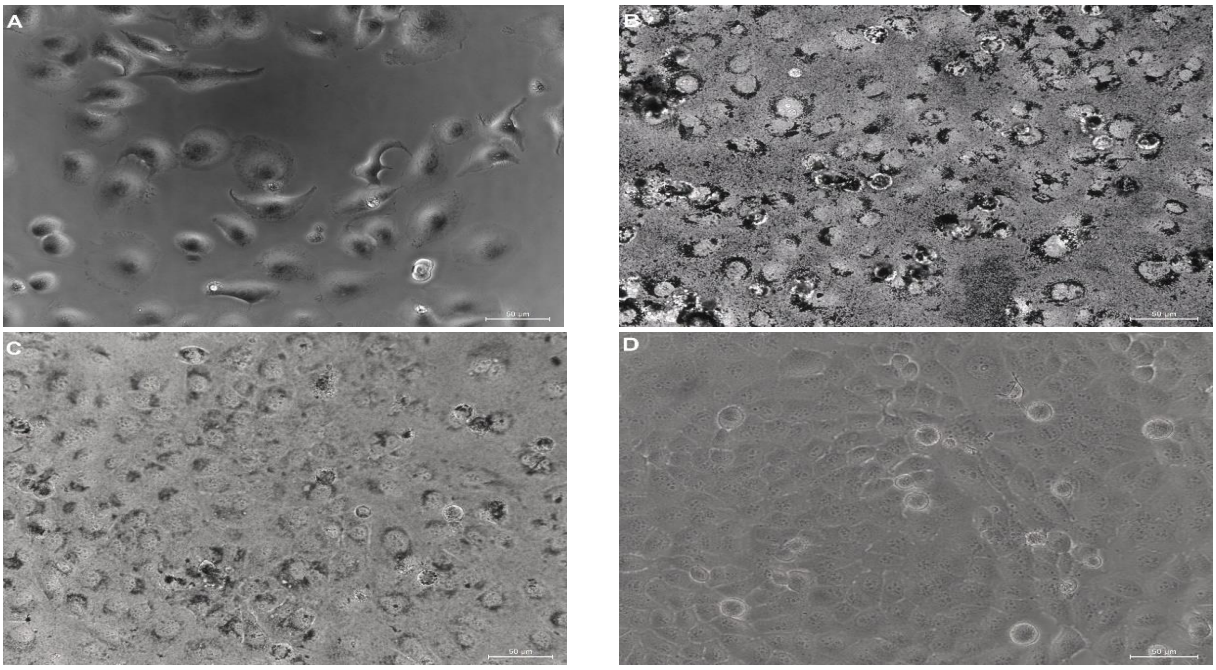

Fig. 7: Optical microscopy of MCF-7 cells lines treated with ks-AuNPs, ks-AgNPs and KS in the concentration of 0.2 mM for 48h, (A) Control cells, (B) ks-AuNPs, (C) ks-AgNPs and (D) KS.

Conclusion

We have shown a green chemistry approach for the synthesis of Ks-AuNPs and ks-AgNPs by using water as solvent and KS alone as the reducing agent. This approach is clean, efficient and eco-friendly without the use of organic solvents and hazardous agent such as sodium borohydride, CTAB, and so forth. The UV-vis spectra revealed the formation and stability of the ks-AuNPs and ks-AgNPs. The TEM, XRD and XPS spectra revealed shape, nanoscale size, crystallinity and chemical environment of synthesized nanoparticles, repectively. The FTIR spectra indicated that the –OH functional groups of KS played an important role in reduction of Au^{3+} and Ag^{+} to AuNPs and AgNPs, respectively. The present study showed potential cytotoxic activities of ks-AuNPs and ks-AgNPs on MCF-7 cells.

Acknowledgments

This study was financially supported by the National Science Foundation of China (No. 21172182 and 21362026). The Author declares no conflict of interest.

References

1. E. Boisselier, D. Astruc, Gold nanoparticles in nanomedicine: preparations, imaging, diagnostics, therapies and toxicity, *Chem. Soc. Rev.* **38**, 1759 (2009).
2. D. A. Giljohann, D. S. Seferos, W. L. Daniel, M. D. Massich, P. C. Patel, C. A. Mirkin, Gold nanoparticles for biology and medicine, *Angew. Chem. Int. Ed*. **49**, 3280 (2010).
3. A. M. Fayaz, K. Balaji, M. Girilal, R. Yadav, P. T. Kalaichelvan, R. Venkatesan, Biogenic synthesis of silver nanoparticles and their synergistic effect with antibiotics: A study against gram-positive and gram-negative bacteria, *Nanomed*. *Nanotechnol*. **6**, 103 (2010).
4. E. Elinav, D. Peer, Harnessing nanomedicine for mucosal theranostics-a silver bullet at last, *ACS Nano*. **7**, 2883 (2013).
5. C. G. Kumar, Y. Poornachandra, S. K. Mamidyala, Green synthesis of bacterial gold nanoparticles conjugated to resveratrol as delivery vehicles, *Colloids Surf. B: Biointerfaces* **123**, 311 (2014).
6. S. Patra, S. Mukherjee, A. K. Barui , A. Ganguly, B. Sreedhar, C. R. Patra, Green synthesis, characterization of gold and silver nanoparticles and their potential application for cancer therapeutics, *Mater. Sci. Eng. C* **53**, 298 (2015).
7. T. Shanmugasundaram, M. Radhakrishnan, V. Gopikrishnan, K. Kadirvelu, R. Balagurunathan, Biocompatible silver, gold and silver/gold alloy nanoparticles for enhanced cancer therapy: in vitro and in vivo perspectives. *Nanoscale* **9**, 16773 (2017).
8. C. E. Benjamin, Z. Chen, P. Y. Kang, B. A. Wilson, N. Li, S. O. Nielsen, Z. P. Qin, J. J. Gassensmith, Site-selective nucleation and size control of gold nanoparticle photothermal antennae on the pore structures of a virus. *J. Amer*. *Chem. Soc*. **140**, 17226

(2018).
9. G. R. Rudramurthy, M. K. Swamy**,** Potential applications of engineered nanoparticles in medicine and biology: an update. *J. Biol. Inorg. Chem.* **23**, 1185 (2018).
10. C. J. Murphy, A. M. Gole, J. W. Stone, P. N. Sisco, A. M. Alkilany, E. C. Goldsmith, S. C. Baxter, Gold nanoparticles in biology: beyond toxicity to cellular imaging, *Acc. Chem. Res.* **41**, 1721 (2008).
11. R. Shukla, S. K. Nune, N. Chanda, K. Katti, S. Mekapothula, R. R. Kulkarni, W. V. Welshons, R. Kannan, K. V. Katti, Soybeans as a phytochemical reservoir for the production and stabilization of biocompatible gold nanoparticles, Small **4**, 1425(2008).
12. N. A. Begum, S. Mondal, S. Basu, R. A. Laskar, B. Mandal, Biogenic synthesis of Au and Ag nanoparticles using aqueous solutions of black tea leaf extracts, *Colloids Surf. B: Biointerfaces* **71**, 113(2009).
13. S. Lokina, A. Stephen, V. Kaviyarasan, C. Arulvasu, V. Narayanan, Cytotoxicity and antimicrobial activities of green synthesized silver nanoparticles, *Eur. J. Med. Chem.* **76**, 256 (2014).
14. R. K. Das, P. Sharma, P. Nahar, U. Bora, Green synthesis of gold nanoparticles using ethanolic leaf extract of Centella asiatica, *Mater. Lett.* **64**, 1445 (2010).
15. P. Elia, R. Zach, S. Hazan, S. Kolusheva, Z. Porat, Z. Yehuda, Green synthesis of gold nanoparticles using plant extracts as reducing agents, *Int. J. Nanomed.* **9**, 4007 (2014).
16. S. Das, J. Chakraborty, S. Chatterjee, H. Kumar, Prospects of biosynthesized nanomaterials for the remediation of organic and inorganic environmental contaminants, *Environ. Sci-Nano* **5**, 2784 (2018).
17. P. K. Rai, V. Kumar, S. Lee, N. Raza, K. H. Kim, Y. S. Ok, D. C. W. Tsang, Nanoparticle-plant interaction: implications in energy, environment, and agriculture, *Environ. Int.* **119**, 1 (2018).
18. K. Sindhu, A. Rajaram, K. J. Sreeramc, R. Rajaram, Curcumin conjugated gold nanoparticle synthesis and its biocompatibility, *RSC Adv.* **4**, 1808 (2014).
19. F. J. Osonga, I. Yazgan, V. Kariuki, D. Luther, A. Jimenez, P. Le, O. A. Sadik, Greener synthesis and characterization, antimicrobial and cytotoxicity studies of gold nanoparticles of novel shapes and sizes, *RSC Adv.* **6**, 2302 (2016).
20. J. M. Calderon–Montano, E. Burgos–Moron, C. Perez–Guerrero, A review on the dietary flavonoid kaempferol, *Mini. Rev. Med. Chem.* **11**, 298 (2011).
21. A. Y. Chen, Y. C. Chen, A review of the dietary flavonoid, kaempferol on human health and cancer chemoprevention, *Food Chem.* **138**, 2099 (2013).
22. P. Rajendran T. Rengarajan, N. Nandakumar, R. Palaniswami, Y. Nishigaki, I. Nishigaki, Kaempferol, a potential cytostatic and cure for inflammatory disorders, *Eur. J. Med. Chem.* **86**, 103 (2014).
23. Y. Zhang, A. Y. Chen, M. Li, C. Chen, Q. Yao, Ginkgo biloba extract kaempferol inhibits cell proliferation and induces apoptosis in pancreatic cancer cells, *J. Surg. Res.* **148**, 17(2008).
24. X. B. Yang, Q. Wang, C. M. Wang, X. L. Qin, Y. Huang, R. Q. Zeng. Synthesis and protective effects of kaempferol–3′–sulfonate on hydrogen peroxide-induced injury in vascular smooth muscle cells, *Chem. Biol. Drug. Des.* **87**, 841 (2016).
25. P. Mulvaney, Surface plasmon spectroscopy of nanosized metal particles, *Langmuir* **12**, 788 (1996).
26. J. Kimling, M. Maier, B. Okenve, V. Kotaidis, H. Ballot, A. Plech, Turkevich method for gold nanoparticle synthesis revisited, *J. Phys. Chem.* **110**, 15700 (2006).
27. S. S. Shankar, A. Rai, A. Ahmad, M. Sastry, Controlling the optical properties of lemon grass extract synthesized gold nanotriangles and potential application in infrared absorbing optical coatings, *Chem. Mater.* **17**, 566 (2005).
28. D. Jain, H. K. Daima, S. Kachhwaha, S. L. Kothari, Synthesis of plant-mediated silver nanoparticles using papaya fruit extract and evaluation of their anti microbial activities, *Digest J Nanomater Biostruct.* **4**, 723 (2009).
29. Y. C. Wang, M. H. Engelhard, D. R. Baer, D. G. Castner, Quantifying the impact of nanoparticle coatings and nonuniformities on XPS analysis: gold/silver core shell nanoparticles, *Anal. Chem.* **88**, 3917 (2016).
30. M. A. Brown, A. B. Redondo, M. Sterrer, B. Winter, G. Pacchioni, Z. Abbas, J. A. van Bokhoven, Measure of surface potential at the aqueous–oxide nanoparticle interface by XPS from a liquid microjet, *Nano Lett.* **13**, 5403 (2013).
31. G. S. Perera, S. A. Athukorale, F. Perez, C. U. Pittman Jr., D. M. Zhang, Facile displacement of citrate residues from gold nanoparticle surfaces, *J. Colloid Interf. Sci.* **511**, 335 (2018).
32. P. Rajasekharreddy, P. U. Rani, Biofabrication of Ag nanoparticles using Sterculia foetida L. seed extract and their toxic potential against mosquito vectors and HeLa cancer cells. *Mater. Sci. Eng. C* **39**, 203 (2014).
33. Z. Krpetic, G. Scarı, C. Caneva, G. Speranza, F. Porta, Gold nanoparticles prepared using cape aloe active components, *Langmuir* **25**, 7217 (2009).